

A Four Element Antenna System with Antenna Diversity for Dual Band WLAN Operation

Yuan-Kai Shih^{#1}, Wen-Jiao Liao[#], Shih-Hsun Chang[#], Ping-Chieh Chiang[#], Chun-Ting Yeh[#], Tzyh-Ghuang Ma[#],

[#]Department of Electrical Engineering, National Taiwan University of Science and Technology

No. 43, Sec 4., Keelung Rd., Taipei 10607, Taiwan (R.O.C.)

¹ j000703@hotmail.com

Abstract—An antenna arrangement made of four similar compact dual-band chip antennas is proposed for uses on WLAN access point devices. The antenna are placed at corners of a small printed circuit board that emulates a WLAN base station. The antenna comprises a feeding line, a clearance region and a chip with a slotted patch. The volume occupied by each antenna chip is $8.5 \times 3 \times 1.6 \text{ mm}^3$ only. Antenna diversity is achieved with a combination of spatial diversity and pattern diversity. Simulation and measurement results demonstrate good isolation performance among antennas. Proposed antenna configuration can also be applied to WLAN devices with the MIMO feature.

I. INTRODUCTION

The deployment of wireless local area network (WLAN), which is also referred as the IEEE 802.11 standard, has achieved a great success in recent years. Almost all mobile communication systems are equipped with some variations of WLAN protocols. Newer versions of WLAN standards are aimed to provide robust operation and enhanced throughput. To accomplish this goal, advanced technologies such as antenna diversity and multi-input multi-output (MIMO) are also included in those standards. In 802.11n, 2×2 and 4×4 MIMO are designated to achieve data rates up to 300 Mbps and 600 Mbps, respectively [1]. As a result, WLAN antennas, especially the ones installed on portable devices, are required to provide more versatile performance features.

Numerous WLAN antenna designs have been proposed and published. Many of them belong to categories such as the planar inverted-F antennas [2], couple-fed PIFA antennas [3], monopole antennas with parasitic elements [4], and shorted T-shaped monopole antenna [5]. Though those designs can operate in WLAN bands and many of them can achieve good radiation efficiencies, proposed antenna configurations usually suffer from large sizes and complicated geometries. Those short comings may prevent their applications on mobile devices, which are getting smaller.

In addition to small form factor and simple antenna structure, WLAN antennas on portable devices are likely to be packed with other antennas. The multiple element antenna system, which has already been adopted in some wireless communication applications, is likely to be installed on more WLAN devices in the future. Previous works have demonstrated that use multiple antennas with different characteristics can help mitigate multipath fading and increase the channel throughput. The larger the number of uncorrelated channels, the higher is the bandwidth.

Three types of antenna diversities are available. They are spatial diversity, pattern diversity, and polarization diversity. Antenna diversity plays an important role for multiple element antenna system. In [6], a cellular phone comprising a PIFA, an IFA, and a monopole is studied. An optimization of integrating a PIFA and an IFA on a phone is provided in [7]. Decoupling measures are implemented for two PIFAs in [8]. A multi antenna system is proposed for access point (AP) in [9]. Reduction in multipath interference using spatial and pattern diversity techniques are discussed in [10].

In this work, a four element antenna system is proposed for the AP device. Primary goals include design a compact dual band WLAN chip antenna and reduce mutual couplings among antennas. In addition to small sizes and good isolation, low fabrication cost and high radiation efficiency are also desired properties. The antenna design was conducted with HFSS simulation, which is based on the finite element method. The proposed design was fabricated and measured to validate its performance. Section II describes the antenna structure and the four element antenna system. Simulated and measured results are compared and analysed in Section III. Section IV provides a brief conclusion.

II. THE 4-ELEMENT ANTENNA SYSTEM

A. Chip Antenna Design

The configuration of the proposed WLAN chip antenna was adopted from [11], which is a dual band GNSS antenna capable of providing circularly polarized radiation. The design was modified to comply with the two WLAN operation bands. The chip antenna is relatively small in terms of sizes, which are $8.5 \text{ mm} \times 3 \text{ mm}$ only. Fig. 1 shows the antenna configuration. The metal patch is laid on a 1.6 mm thick FR4 substrate. The chip is placed at the corner of a test bench, which emulates the AP device. Sizes of the metal ground are $50 \text{ mm} \times 50 \text{ mm}$. A clearance region of $20 \text{ mm} \times 6 \text{ mm}$ is cut on the corner to accommodate the antenna chip. Detailed geometric parameters are listed in Table I.

As shown in Fig. 1, the antenna comprises four parts: the metal patch on the chip, the etched slit on the patch, the clearance region, and a feed strip. A slanted 50 Ohms microstrip line on the ground connects the feed strip to an SMA connector. Note that no matching network is needed since the antenna itself already provides good matching in the two operation bands.

B. Parametric Studies of Key Antenna Design Parameters

Parametric studies were conducted via simulations to verify the antenna performance. The results provide design guidelines which are useful when transporting the design to platforms of different sizes. Impedance matching can be tuned using critical design parameters.

According to [11], the feed strip is an important source for radiation. The antenna's matching condition is also sensitive to the sizes of the feed strip. Fig. 2 provides a comparison of reflection coefficient spectra of different feed strip widths. It has a great impact on the upper band resonance.

The clearance region length and width are also essential to impedance matching. Simulation results suggest the clearance region length affects the upper band impedance, while the clearance region width also changes the resonance frequency.

The length of the patch's end section L_{z2} was also studied. Its main impact is on the lower band resonance frequency, which is inversely proportional to the end section length. Optimal design parameters are listed in Table I.

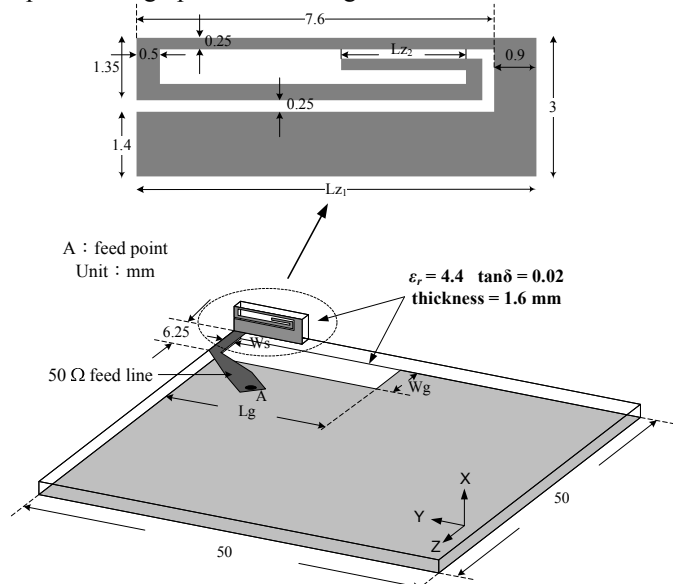


Fig. 1. Detailed geometry of the proposed dual band WLAN antenna.

TABLE I

DIMENSIONS OF THE PROPOSED DUAL BAND WLAN ANTENNA.

L_g	L_{z1}	L_{z2}	W_g	W_s
20	8.5	2.65	6	1.5

Unit: mm

C. Four Antenna Arrangement

In order to provide antenna diversity for the AP device, four identical antenna chips are placed at corners of a square platform. Fig. 3 shows the proposed 4 element antenna system. Antenna diversity can be achieved in terms of spatial and pattern diversities. The reflection coefficient spectra of the four antennas are almost identical, and are similar to the one of a single antenna on the platform. Couplings among antennas are examined via transmission spectra, which are shown in Fig. 4. S21 and S41 curves have no difference since geometric relationship between Antenna #2 and #1 is the same as the one between Antenna #1 and #4. The S31 curve is even

lower since the distance between Antenna #3 and #1 is longer. Note transmission coefficients are higher in antenna's resonant bands. This suggests that low transmission coefficients among antennas are mainly suppressed by spatial separation.

The antenna diversity can be evaluated via envelop correlation coefficient (ECC) ρ_e , which is defined as (1) [12]. This is commonly used for multi element antenna systems since only S-parameters are involved. Table II lists in-band ECC values of Antenna #1 toward the other 3 antennas. The values are very small, indicating that there are certain antenna diversities among antennas on the AP platform.

$$\rho_e = \frac{|S_{11}^* S_{12} + S_{21}^* S_{22}|^2}{(1 - |S_{11}|^2 - |S_{21}|^2)(1 - |S_{22}|^2 - |S_{12}|^2)} \quad (1)$$

TABLE II
CALCULATED CORRELATION COEFFICIENTS. (ρ_e)

	Ant. 1 & Ant. 2	Ant. 1 & Ant. 3	Ant. 1 & Ant. 4
WLAN (2.4~2.48 GHz)	0.001296	0.000304	0.001235
Hyper LAN (5.15~5.85 GHz)	0.000337	0.000308	0.00035

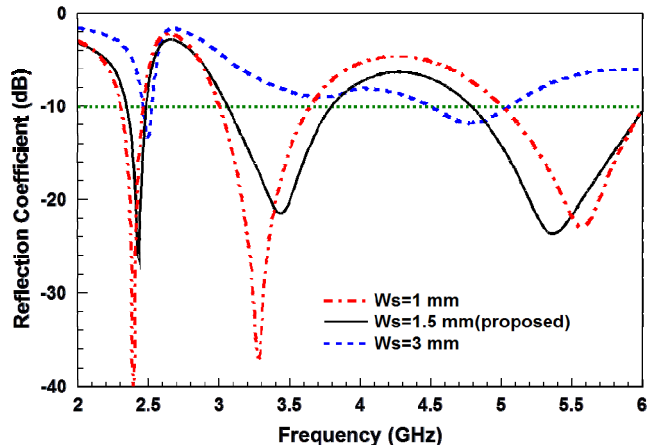


Fig. 2. Comparison of impedance matching of various strip line widths.

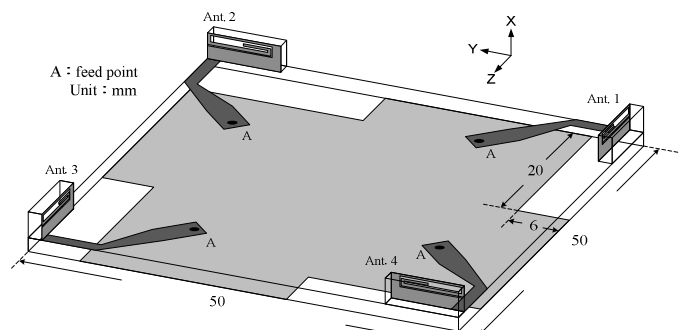


Fig. 3. Configuration of the four antennas arrangement.

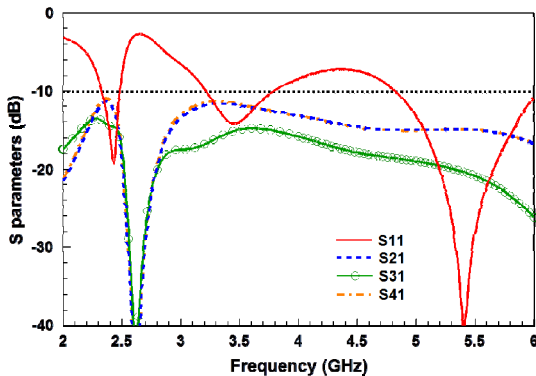


Fig. 4. Simulated isolation between four antennas.

III. ANTENNA PERFORMANCE VALIDATION

The proposed design was fabricated via the etching process on printed circuit boards. Fig. 5 shows the prototype of the 4-element antenna system. SMA connectors were soldered to the back to provide connections. Antenna performances were evaluated via S-parameter and pattern measurements.

A. S-Parameters

Measured reflection coefficient shown in Fig. 6 in general agrees with the simulated one, especially in WLAN operation bands. Other three antennas on the platform exhibit the same matching performance. Measured coupling spectra shown in Fig. 7 are also similar to simulated ones illustrated in Fig. 4. The worst in-band isolation observed is about 13 dB, which is due to the close spacing in the 2.4 GHz band. The 50 mm separation is less than a half wavelength. In the 5 GHz hyper LAN band, the in-band isolation is improved to 16 dB.

B. Radiation Pattern

The prototype antenna was placed in a 3D spherical near field chamber to measure its radiation features. Fig. 8 provides comparisons of measured and simulated total radiation patterns on principle planes at 2.45 and 5.5 GHz. The lower band patterns are somewhat different. The null on the simulated yz -plane plane disappears in the measured pattern. During measurements, we observed that there are substantial return currents flowing on the coaxial cable connecting to the SMA connector. This is due to the unbalanced feed structure. These currents also contribute to radiation and hence interferes the pattern. In order to suppress radiation from the cable, absorber was wrapped around the cable. Nevertheless, the residual current on the cable still alter patterns in a certain degree. On the other hand, the difference in the upper band is not that much. Similar patterns are observed in simulated and measured results. Note that in measured patterns, there are nulls in the $-z$ axis direction in both bands. This is because the turn table in the spherical chamber prevents the sampling probe from entering the region underneath the antenna. Some errors were incurred in this region.

Radiation patterns of the four antennas installed on the platform are shown in Fig. 9. The 3D patterns shown indicate the beams are leaning toward different directions, which contribute to pattern diversity. Measured maximum gains and

radiation efficiencies in the antenna's two operation bands are plotted in Fig. 10. Those radiation performances are rather stable. The maximum gains are around -1 and 3 dBi in the lower and upper bands, respectively. As to the radiation efficiency, it is about 40% in the 2.4 GHz band, and is increased to 70% in the hyper LAN band. Those lower band efficiency is somewhat small due to compact antenna sizes.



Fig. 5. Fabricated dual band WLAN antenna and the 4 antenna arrangement.

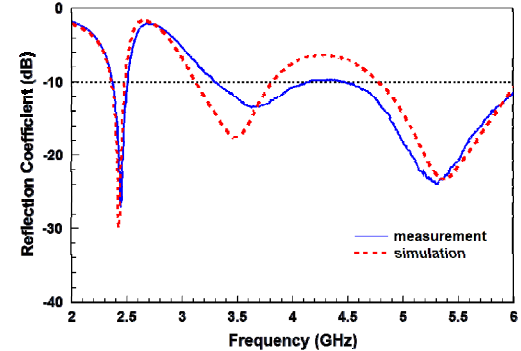


Fig. 6. Comparison of simulated and measured reflection coefficient spectra of the proposed dual band WLAN chip antenna.

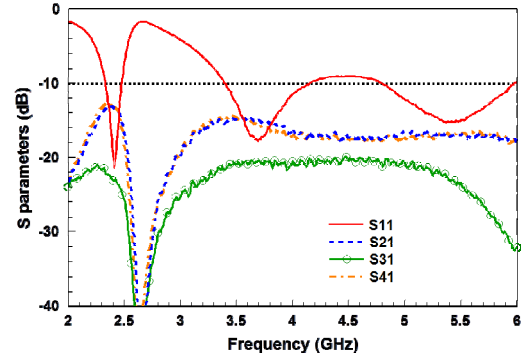
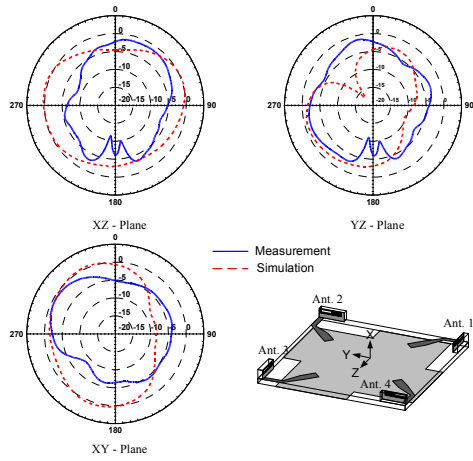


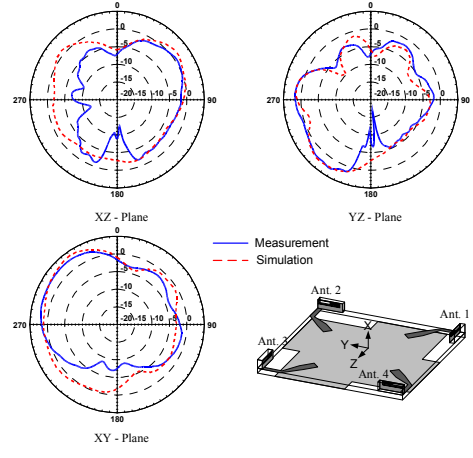
Fig. 7. Measured isolation between the four antennas on the platform.

IV. CONCLUSION

A multi element antenna system containing four dual band WLAN antennas is proposed in this work. The antenna sizes are $8.5 \text{ mm} \times 3 \text{ mm} \times 1.6 \text{ mm}$ only. Measurements were conducted to verify that its operation bands comply with IEEE 802.11 standard requirements. In-band radiation efficiencies are maintained above 40%. The antenna diversity of the 4 element system is realized via pattern and spatial diversities. Due to small sizes of the projected AP platform, the lower band isolation performance is limited. On the other hand, good decoupling performance is achieved in the upper hyper LAN band. As to future work topics, existing decoupling methods can be implemented to the 4-element system to further improve its antenna diversity performance.

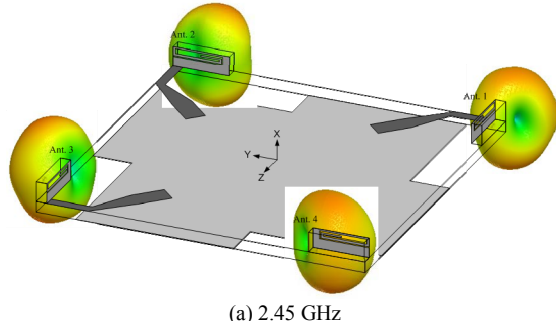


(a) 2.45 GHz

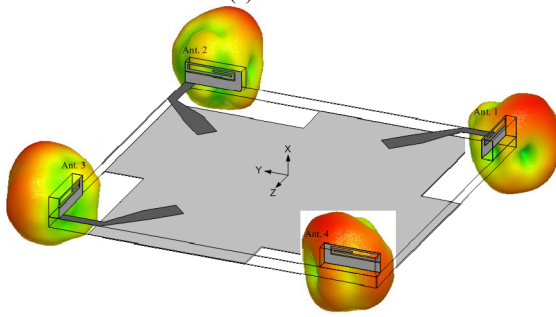


(b) 5.5 GHz

Fig. 8. Measured gain power patterns of Antenna 1 on principle planes.



(a) 2.45 GHz



(b) 5.5 GHz

Fig. 9. Simulated 3D patterns of four antennas.

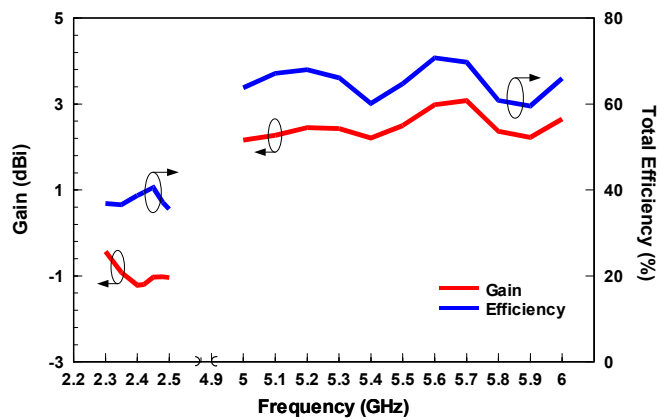


Fig. 10. Measured gain and total efficiency spectra of Antenna 1.

REFERENCES

- [1] Buffalo Technology, "Understanding and Optimizing 802.11n," Internet: http://www.lmi.net/wp-content/uploads/Optimizing_802.11n.pdf, [Nov. 11, 2012].
- [2] T. Hosoe and K. Ito, "Dual-band planar inverted F antenna for laptop computers," *IEEE Antennas Propag. Int. Symp.*, vol. 3, pp. 87-90, Jun. 2003.
- [3] C.-T. Lee and K.-L. Wong, "Uniplanar printed coupled-fed PIFA with a band-notching slit for WLAN/WiMAX operation in the laptop computer," *IEEE Trans. Antennas Propag.*, vol. 57, no. 4, pp. 1252-1258, Apr. 2009.
- [4] K.-L. Wong, L.-C. Chou, and C.-M. Su, "Dual-band flat-plate antenna with a shorted parasitic element for laptop applications," *IEEE Trans. Antennas Propag.*, vol. 53, No. 1, pp. 539-544, Jan. 2005.
- [5] C.-M. Su, W.-S. Chen, and K.-L. Wong, "Metal-plate shorted T-shaped monopole for internal laptop antenna for 2.4/5 GHz WLAN operation," *IEEE Antennas Propag. Int. Symp.*, vol. 2, pp. 1943-1946, Jun. 2004.
- [6] B.-T. Jiang, J.-F. Mao, "Design of an PIFA-IFA-monopole in dual-SIM mobile phone for GSM/DCS/Bluetooth operation," *ICMPT Proceedings.*, vol. 3, pp. 1050-1053, Apr. 2008.
- [7] Z. Li, and S.-Y. Rahmat, "Optimization of PIFA-IFA combination in handset antenna designs," *IEEE Trans. Antennas Propag.*, vol. 53, no. 5, pp. 1770-1778, May 2005.
- [8] A. Diallo, C. Luxey, T.-P. Le, R. Staraj, and G. Kossiavas, "Study and reduction of the mutual coupling between two mobile phone PIFAs operating in the DCS1800 and UMTS bands," *IEEE Trans. Antennas Propag.*, vol. 54, no. 11, pp. 3063-3074, Nov. 2006.
- [9] S.-W. Su, "High-gain shorted monopole antennas for concurrent access-point applications," *IEEE Antennas Propag. Int. Symp.*, pp. 1-4, Jul. 2010.
- [10] Y. Ding, Z. Du, K. Gong, and Z. Feng, "A novel dual-band printed diversity antenna for mobile terminals," *IEEE Trans. Antennas Propag.*, vol. 55, no. 7, pp. 2088-2096, Jul. 2007.
- [11] J1. S.-H. Chang, W.-J. Liao, "A novel dual band circularly polarized GNSS antenna for handheld devices," Accepted by *IEEE Trans. Ant. Propag.*, scheduled to be published on vol. 61, no. 2, Feb. 2013.
- [12] J. Avendal, Z. Ying, and B.-K. Lau, "Multiband diversity antenna performance study for mobile phone," *Proceedings IEEE IWAT.*, pp. 193-196, Mar. 2007.